Journal of Nuclear Medicine, published on December 5, 2019 as doi:10.2967/jnumed.119.236083

Quantitative test-retest measurement of ^{68}Ga-PSMA-HBED-CC (PSMA-11) in tumor and normal tissue

Authors:

Janet H Pollard MD[1,2], Caleb Raman[3], Yousef Zakharia MD[4], Chad R Tracy MD[5], Kenneth G. Nepple MD[5], Tim Ginader MS[6], Patrick Breheny PhD[7] John J Sunderland PhD[1]

Author affiliations:

[1]Department of Radiology, University of Iowa Carver College of Medicine, Iowa City, Iowa

[2]Iowa City Veterans Healthcare Center, Iowa City, Iowa

[3]College of Arts and Sciences, University of Iowa, Iowa City, Iowa

[4]Department of Internal Medicine, University of Iowa Carver College of Medicine, Iowa City, Iowa

[5]Department of Urology, University of Iowa Carver College of Medicine, Iowa City, Iowa

[6]Biostatistics Core, University of Iowa Carver College of Medicine, Iowa City, Iowa

[7]Department of Biostatistics, University of Iowa College of Public Health, Iowa City, Iowa

Disclaimer: None

Corresponding author:

Janet H Pollard,

Department of Radiology

Division of Nuclear Medicine

200 Hawkins Drive

Iowa City, IA 52242-1077

Phone#: 319-356-1259

Fax#: 319-356-2220

Email: janet-pollard@uiowa.edu

First author:

Janet H Pollard, Clinical Assistant Professor of Radiology

Department of Radiology

Division of Nuclear Medicine

200 Hawkins Drive

Iowa City, IA 52242-1077

Phone#: 319-356-1259

Fax#: 319-356-2220

Email: janet-pollard@uiowa.edu

Financial disclosure:

Dr. Pollard is an investigator for Progenics and Endocyte (Advanced Accelerator Applications/Novartis). The authors of this article have indicated no other relevant relationships that could be perceived as a real or apparent conflict of interest.

Word count: 5000/5000

Running title: Repeatability of ^{68}Ga-PSMA-HBED-CC

ABSTRACT

The PET radiotracer ^{68}Ga-PSMA-HBED-CC (^{68}Ga-PSMA-11) shows potential as an imaging biomarker for recurrent and metastatic prostate cancer. The purpose of this study was to determine repeatability of ^{68}Ga-PSMA-HBED-CC in a test-retest trial in subjects with metastatic prostate adenocarcinoma. Methods: Subjects with metastatic prostate cancer underwent two PET/CT scans with ^{68}Ga-PSMA-HBED-CC within 14 days (mean 6 ± 4 d). Lesions in bone, nodes, prostate/bed, and visceral organs as well as representative normal tissues (salivary glands and spleen) were segmented separately by two readers. Absolute and percent differences in SUV_{max} and SUV_{mean} were calculated for all test-retest regions. Repeatability was assessed using percentage difference, within-subject coefficient of variation (wCV), repeatability coefficient (RC), and Bland-Altman analysis. Results: 18 subjects were evaluated, 16 of which demonstrated local or metastatic disease on ^{68}Ga-PSMA-HBED-CC PET/CT. A total of 136 lesions were segmented in bone (n=99), nodes (n=27), prostate/bed (n=7), and viscera (n=3). The wCV for SUV_{max} was 11.7% for bone lesions and 13.7% for nodes. The RC was ±32.5% SUV_{max} for bone lesions and ±37.9% SUV_{max} for nodal lesions, meaning 95% of the normal variability between two measurements will be within these numbers, so larger differences are likely attributable to true biological changes in tumor rather than normal physiologic or measurement variability. wCV in the salivary glands and spleen was 8.9% and 10.7% SUV_{mean}, respectively. Conclusions: Repeatability measurements for PET/CT test-retest with ^{68}Ga-PSMA-HBED-CC show a wCV 12-14% SUV_{max} and RC ±33-38% SUV_{max} in bone and nodal lesions. These estimates are an important aspect of ^{68}Ga-PSMA-HBED-CC as a quantitative imaging biomarker. These estimates are similar to those reported for ^{18}F-FDG, suggesting that ^{68}Ga-PSMA-HBED-CC PET/CT may be useful in monitoring response to therapy.

Keywords: repeatability, SUV, PSMA HBED-CC, PSMA-11, PET/CT

INTRODUCTION

Quantitative PET imaging of prostate cancer has the potential to influence management in the setting of response-to-treatment and radiation dose estimation of both tumor and critical organs in targeted radionuclide therapy. Development of a quantitative imaging biomarker such as ^{68}Ga-PSMA HBED-CC requires an understanding of the biomarker's technical performance, including estimates of measurement linearity, bias, error, repeatability, and reproducibility (*1,2*). Measurement error or variability in measurement of radiotracer performance derives from many sources including aspects of patient preparation and physiology, the imaging system, and measurement methodology. Repeatability, as an estimate of the magnitude of change that distinguishes normal physiologic and measurement variability from true biological change, is important to the interpretation of changes encountered on PET scans in the response-to-treatment setting. Understanding baseline variability of measurement has similar utility in dose estimation in theranostic applications. In this prospective study we report estimates of repeatability for ^{68}Ga-PSMA-HBED-CC PET/CT in patients with metastatic prostate cancer.

MATERIALS AND METHODS

Study Design and Patient Population

The study was a prospective, single-institution trial consisting of a test-retest methodology. Subjects each underwent two ^{68}Ga-PSMA-HBED-CC PET/CT scans no less than 12 hours and no greater than 14 days apart. Strict attention was given to subject preparation and scan acquisition to assure near identical imaging conditions. This included injected activity, radiotracer uptake time, and consistency of scanner selection and scan technique for each subject.

Eighteen subjects with castrate sensitive or castrate resistant prostate cancer were enrolled. Of these, 16 subjects demonstrated local or metastatic disease on ^{68}Ga-PSMA-HBED-CC PET/CT. All but 2 subjects had histologic confirmation of prostate adenocarcinoma from primary or metastatic lesions; two subjects were diagnosed based on clinical presentation, elevated prostate specific membrane antigen (PSA), and widespread metastatic disease on conventional imaging. Individual and group characteristics are listed in Table 1. Subjects had ≥ 2 metastatic sites on conventional imaging (bone scan, CT, or MRI). To avoid changes in tumor due to therapy, subjects could not undergo prostate cancer therapy administration between the two exams, and were not enrolled within three months of starting hormonal or chemotherapy. Subjects' systemic therapy regimens are listed in Supplemental Table 1.

The study (NCT02952469) was approved by the institutional review board and radioactive drug research committee (RDRC). Enrollment was voluntary. Subjects were compensated $60 total for the two study visits. All subjects signed an informed consent form. Periodic safety assessments were performed as required per protocol under the RDRC with the Food and Drug Administration.

^{68}Ga-PSMA-HBED-CC Synthesis

^{68}Ga-PSMA-HBED-CC was manufactured on-site on the same day as the PET/CT scans. ^{68}Ga was obtained from an on-site ^{68}Ge/^{68}Ga generator (IGG100, Eckert-Ziegler, Berlin, Germany). Radiolabeling was performed using an automated Modular Lab PharmTracer synthesis module (Eckert & Ziegler Eurotope, Berlin). The synthesis process was conducted in a sterile cassette system specifically designed for ^{68}Ga-PSMA-HBED-CC (Eckert & Ziegler Eurotope, Part # C4-GA68-PSMA) using the acetone-free method (*3*).**Scan Acquisition and Reconstruction**

Target administered activity was 129.5 MBq (3.5 mCi) followed by target uptake time of 60 minutes. Each subject's scans were performed on the same PET/CT scanner, either a Siemens mCT with FlowMotion (n=11) or Siemens Biograph Truepoint (n=7) (Siemens Healthcare, Germany). Scans covered skull vertex to midthigh with 3-4 minutes per bed position or the equivalent. mCT images were reconstructed onto a 200 x200 matrix with 3.4mm pixels using 3D ordered subset expectation maximization (OSEM) with Time of Flight, and a 5mm Gaussian filter, while the Biograph TruePoint images were 168 x 168 with 3.4mm pixels reconstructed with 3D OSEM using 4 iterations, 8 subsets and a 7mm filter.

Lesion Selection and Segmentation

Images were analyzed using MIM Encore (MIM Software Inc, Cleveland, OH). Initial segmentation was performed with MIM's semi-automated PET Edge® tool which uses a gradient-based technique to detect the steepest drop off in SUV values (Fig. 1). However, manual intervention with contours was still a significant part of the segmentation process, introducing intra-reader and inter-reader measurement variability. Two readers were used: a nuclear radiologist (JHP) and a research assistant (CR) trained in use of the software and in recognition of anatomic structures and pathologic lesions. Both readers located and segmented all lesions and organs. All volumes of interest (VOI) were reviewed together to resolve major discrepancies in organ and lesion selection and contours.

The spleen and salivary glands were measured and analyzed, first individually, then later pooled together (for the salivary glands) for global repeatability. Up to 15 total bone lesions per subject were selected from across five skeletal regions consisting of 1) skull; 2) thorax (ribs, sternum, clavicles, and scapulae); 3) spine (cervical, thoracic, and lumbar); 4) pelvis (sacrum and pelvic bones); and 5) extremities. Lesions were selected if they were both high in uptake (i.e.

higher than adjacent background activity) and discrete, such that the PET margins were visually identifiable to minimize interobserver variability relating to lesion segmentation. All discrete soft tissue lesions (lymph nodes, prostate/prostate bed, and viscera) were included except for large irregular conglomerate abdominal nodal masses in subject 8.

Soft tissue and bone lesions of all sizes were included. Lymph node size (long axis) was measured on the CT. Defined categories for lymph nodes were < 1.0 cm, 1.0 - 1.5 cm, and > 1.5 cm. Although many bone lesions could not be precisely demarcated on CT, lesion size was approximated from the PET-avid VOI. Two size categorizations for bone lesions were established: 1) VOI < 1.0 mL and ≥ 1.0 mL, and 2) VOI < 1.5 mL, 1.5 - 8.0 mL, > 8.0 mL.

Statistical Analysis

The sample size of this study was 16 subjects. Preliminary sample size calculations indicated that between 14-22 subjects would be needed for an 80-90% probability of estimating repeatability of ^{68}Ga-PSMA-HBED-CC to within 25% accuracy.

Activity concentrations for lesions and organs of interest were expressed as standardized uptake values (SUV) normalized to patient body weight. Metrics included SUV maximal intensity pixel (SUV_{max}) and mean SUV (SUV_{mean}). In each subject the two readers' measurements of each lesion and organ were averaged together for scan 1 and were compared to similarly averaged measurements for scan 2. Data were also pooled and analyzed based on organ and lesion location. Data were also pooled relative to scanner type and analyzed for significant difference.

Repeatability metrics were calculated as described by Lodge and Obuchowski and are listed below (*4,5*):

$$D = \frac{(SUV1-SUV2)}{(SUV1+SUV2)/2} \times 100\% \qquad \text{Equation 1}$$

$$wCV = (SDof\ D)\ /\sqrt{2} \qquad \text{Equation 2}$$

$$RC = 1.96 \times \sqrt{2} \times wCV \qquad \text{Equation 3}$$

$$LRC = \frac{-RC}{1+(RC/200\%)} \qquad \text{Equation 4}$$

$$URC = \frac{RC}{1-(RC/200\%)} \qquad \text{Equation 5}$$

Relative difference (D) in SUV_{max} or SUV_{mean} between scan 1 and scan 2 for each measured site was calculated as in Equation 1. Within-subject coefficient of variation (wCV) was calculated based on the standard deviation (SD) of D over all subjects for each category of lesion or organ measured as in Equation 2. The repeatability coefficient (RC) was calculated using symmetric limits as in Equation 3. The RC or "limit of true change" is a threshold such that 95% of the normal variability between two SUV measurements will be within these numbers, so larger differences in scans are likely attributable to true disease progression or regression. Asymmetric lower and upper RC values (LRC, URC) were calculated as in Equation 4 and Equation 5. Asymmetric RCs have been promoted as the preferred approach when comparing SUV values between baseline and follow-up scans. Weber et al. provide an explanation of the rationale for this approach (*4-7*).

The original measurements, not absolute values, were used to calculate *D, wCV*, and *RC*. The 95% confidence intervals around the RC were calculated assuming normal distribution. Scatter diagrams with linear regression were plotted for SUV_{max} and SUV_{mean} for scan 1 and scan 2 measurements. Bland-Altman plots were created for both the absolute and relative percentage differences for our data. Bias, upper and lower limits of agreement, and Kendall's τ with *p* values were calculated as described in the literature (*4,8,9*). Levene and Breusch-Pagan tests for

equality of variance were used to test for significance for differences in repeatability metrics based on categorical and continuous variables, respectively. Statistical analyses were performed using SAS/STAT software version 9.4 (SAS Institute Inc., Cary, NC, USA) and Microsoft Excel 2016 version 1811.

RESULTS

No adverse events attributable to the radiotracer were observed during the trial. Procedural protocol was rigorously followed for each subject's scan session. Mean time interval between scans was 5.8 ± 3.9 days (range 2-14 days, median 5.5 days, mode 2 days), and was 7 days or less in 14 subjects. There was no significant difference in mean uptake time or injected activity between scan 1 and scan 2. Uptake time ranged from 60-63 min for scan 1 (mean 60.6 ± 1.1 min, 95% CI [60.1, 61.1]) and 60-64 min for scan 2 (mean 60.7 ± 1.2 min, 95% CI [60.1, 61.2]) with P = 0.9. Injected activity ranged from 121.7-145.4 MBq for scan 1 (mean 133.1 ± 7.1 MBq, 95% CI [129.9, 136.4]) and 121.4-146.2 MBq for scan 2 (mean 133.1 ± 6.5 MBq, 95% CI [130.2, 136.0]) with P = 1.0.

Out of 18 enrolled subjects, 16 showed radiotracer-avid disease. Total of 136 lesions were identified and measured. The most common lesions were in the bones (72%, n=99/136), followed by lymph nodes (20%, n=27/136), prostate or prostate bed lesions (5%, n=7/136), and visceral lesions (2%, n=3/136), all from the same subject). The spectrum of lesions in any given subject varied from none to innumerable. Radiotracer-avid lymph nodes were present in only 6 subjects, and most of these lesions were collected from a single subject with predominantly soft tissue disease (Fig. 2). As the VOIs were cross-checked between readers to assure segmentation of the same lesions, interobserver variability was not formally analyzed.

Linear regression demonstrated excellent correlation of SUV measurements between scans (Fig. 3). The wCV, symmetric and asymmetric RC, and 95% confidence intervals for lesions and organs are summarized in Table 2 and Table 3. Bone lesions overall showed wCV 12% and asymmetric limits of RC -28 and +39%. Lymph node lesions overall showed wCV 14% and asymmetric limits of RC -32% and +47%. No significant differences in repeatability were noted based on 1) tissue type (soft tissue versus bone), 2) bone lesion location, 3) bone lesion volume, 4) lymph node size, 5) salivary gland location (parotid versus submandibular), and 6) PSA level (Fig. 4). No significant differences were noted in repeatability based on the type of scanner used; this result is consistent with in-house phantom studies demonstrating scanner model-based repeatability contributions similar between scanners and to be small compared to our measured wCV. Repeatability stratified by scanner type is presented in Supplemental Tables 2 and 3.

Bland Altman plots (Fig. 5 A-D) did not suggest an association between test-retest relative percentage SUV differences and SUV intensity for any measured sites, indicating that the repeatability would be equally reliable for tumors across a wide range of SUV values. This was confirmed by Kendall's τ coefficient analysis (τ and *P* values reported in Fig. 5), which showed no statistically significant association.

DISCUSSION

In this prospective test-retest study we report repeatability for ^{68}Ga-PSMA-HBED-CC PET/CT both for tumor lesions and normal organs (salivary glands and spleen). The repeatability estimates from this study are similar to those reported for FDG, suggesting that ^{68}Ga-PSMA-HBED-CC may be similarly useful as a quantitative imaging biomarker (*10*).

Given the similarities in biodistribution of the small molecule urea-based PSMA-targeting radiotracers our repeatability data for ^{68}Ga-PSMA-HBED-CC may also be applicable to ^{18}F-DCFPyL (*11*). Sahakyan et al. have reported intrasubject repeatability for ^{18}F-DCFPyL in normal organs, but with the limitations of 6 month time intervals and with some patients receiving therapy between scans (*12,13*). Differences in statistical methodologies also makes comparison of results with this work problematic.

In this study we followed a design and statistical methodology described in the literature for ^{18}F-FDG and other PET radiotracers (*1,2,4,5,14*). The performance profile and utility of quantitative ^{18}F-FDG PET for assessment of therapy response for multiple types of tumors is well established, with reported wCV of 10-12% and RC 10-40% (*5-7,10,15-18*). Lodge reviewed the repeatability literature for ^{18}F-FDG, and after reconciling differences in statistical methodology across multiple studies, inferred an average wCV of 10% across all SUV measures (SUV_{max}, SUV_{mean}, and SUV_{peak}), specifically for SUV_{max}, the range of inferred wCV was 5% to 18% (4). As far as the significance of a change for an individual lesion, the RC, also known as limits of true change, are more apt. Lodge estimated RC ±28%, meaning that a lesion that drops in SUV by 28% is likely to represent true change rather than normal variability. Taking into account repeatability and reproducibility data for ^{18}F-FDG, PERCIST 1.0 proposed ± 30% change in SUV for the threshold of change beyond which a tumor can be said to have responded or progressed (*4,15,19*).

Repeatability has also been reported, though not as thoroughly, for other PET radiotracers. Kenny et al. estimated wCV of 9% for ^{11}C-choline in breast cancer (20). Lin et al. estimated wCV of 12% and 14% at the subject level and lesion level, respectively, for ^{18}F-NaF in prostate cancer (*21*). Menda et al. determined that ±25% change in SUV_{max} for neuroendocrine tumors imaged with ^{68}Ga-DOTATOC indicated a true change greater than the measurement error

(*22*). Kramer et al. performed a meta-analysis and estimated a pooled RC of ±25% for solid tumors imaged with ^{18}F-fluorothymidine (*23*).

Variability in PET/CT can arise from a variety of tumor-related, patient-related and external sources. Evolving tumor biology (growth or regression) and medication-induced changes were minimized in this study through the design with short scanning intervals and exclusion of subjects receiving therapy between scans or starting prostate cancer therapy within 3 months of enrollment. Although our subjects were non-fasting as per published guidelines for ^{68}Ga-PSMA PET/CT, we note that Wondergem et al. reported a 13% reduction in uptake of ^{18}F-DCFPyL in the submandibular glands in a cohort of fasting patients as compared to non-fasting patients. They conclude that the effects of fasting are likely negligible in the diagnostic setting, but may need to be investigated further especially in the setting of pre-therapy dosimetry given the impact of PSMA-targeting agents on salivary glands (*24,25*). No diuretics were used in our study, minimizing any effects of hydration status on uptake variability. Strict attention to timing and scanning parameters minimized variability related to technical factors. Lesion segmentation was a source of variability as it relied in part on manual contouring. Interobserver variability, although not formally calculated, was probably a source of error when SUV_{mean} was used, due to the manual involvement of each reader in defining the VOI; however, this was not a source of error when SUV_{max} was used as the highest SUV pixel within a VOI is identical regardless of the size of the VOI.

We hypothesized that lesion size would influence repeatability, however, there appeared to be no significant influence based on bone lesion size. Reliability of this finding is uncertain, as only 17 bone lesions >8.0 mL were evaluated as compared to 82 bone lesions ≤8.0 mL. Similarly, for nodal lesions there was no influence on repeatability based on size, however only 5 nodal lesions >1.5 cm were measured as compared to 22 nodal lesions ≤1.5 cm. Frings et al.

reported better repeatability (less variability) for larger lesion lesions (>4.2 mL versus ≤4.2 mL) for ^{18}F-FDG and ^{18}F-FLT in non-small cell lung cancer, which they attributed to difference in partial volume effects (*26*).

Our study has limitations. Because our scans were performed with the utmost care in patient preparation and scanning parameters, the repeatability estimates derived from our data may be less generalizable to the normal workaday clinic. The interval between the two scans was 7 days or less for most subjects, assuming tumors would be essentially unchanged in volume during this time. Although a shorter maximal timeframe would be preferable in all subjects to assure tumor stability, this was not practicable due to the radiotracer production timetable at our facility and the relatively rural setting with long travel distances for subjects. Whether our repeatability estimates for ^{68}Ga-PSMA-HBED-CC are generalizable to other PSMA-targeting radiotracers such as ^{18}F-DCFPyL is uncertain, but plausible given their similarities in biodistribution. Another limitation is that our data derive from a group of patients with inhomogeneous distribution of metastases. That is, patients with heavy disease burden contributed more lesions to the analysis than did those with few lesions.

CONCLUSION

This study evaluated the repeatability of ^{68}Ga-PSMA-HBED-CC PET/CT in a prospective test-retest design. The wCV for bone and nodal lesions ranged from 12-14% SUV_{max}. RC for bone lesions was approximately ±33% SUV_{max} (asymmetric limits, -28% and +39%) and for nodal lesions was ±38% SUV_{max} (asymmetric limits -32% and +47%). This means that in a potential treatment response setting, SUV changes of a magnitude greater than the RC would indicate with 95% confidence that true change in tumor uptake has occurred rather than measurement error. These findings are similar to those reported for ^{18}F-FDG, suggesting ^{68}Ga-PSMA-HBED-CC

may be suitable for monitoring response to therapy and developing meaningful organ dose estimates in patients with prostate cancer.

KEY POINTS

QUESTION: What is the estimated repeatability of SUV measures on ^{68}GaPSMA HBED-CC PET/CT in patients with metastatic prostate cancer?

PERTINENT FINDINGS: This prospective test-retest study evaluated repeatability of SUV metrics in metastatic lesions and select normal organs. In bone and nodal lesions we found wCV 12-14% SUV_{max} and RC ±33-38 SUV_{max}.

IMPLICATIONS FOR PATIENT CARE: This study is an essential step in the development of ^{68}Ga PSMA HBED-CC PET/CT as a quantitative imaging biomarker and suggests that this radiotracer may be useful for monitoring response to treatment.

REFERENCES

1. Raunig DL, McShane LM, Pennello G, et al. Quantitative imaging biomarkers: a review of statistical methods for technical performance assessment. *Stat Methods Med Res*. 2015;24(1):27-67.

2. Kessler LG, Barnhart HX, Buckler AJ, et al. The emerging science of quantitative imaging biomarkers terminology and definitions for scientific studies and regulatory submissions. *Stat Methods Med Res*. 2015;24(1):9-26.

3. Schultz MK, Mueller D, Baum RP, Watkins GL, Breeman WA. A new automated NaCl based robust method for routine production of gallium-68 labeled peptides. *Appl Radiat Isot*. 2013;76:46-54.

4. Lodge MA. Repeatability of SUV in Oncologic (18)F-FDG PET. *J Nucl Med*. 2017;58(4):523-532.

5. Obuchowski NA. Interpreting Change in Quantitative Imaging Biomarkers. *Acad radiol*. 2018;25(3):372-379.

6. Weber WA, Gatsonis CA, Mozley PD, et al. Repeatability of 18F-FDG PET/CT in Advanced Non-Small Cell Lung Cancer: Prospective Assessment in 2 Multicenter Trials. *J Nucl Med*. 2015;56(8):1137-1143.

7. Velasquez LM, Boellaard R, Kollia G, et al. Repeatability of 18F-FDG PET in a multicenter phase I study of patients with advanced gastrointestinal malignancies. *J Nucl Med*. 2009;50(10):1646-1654.

8. Bland JM, Altman DG. Statistical methods for assessing agreement between two methods of clinical measurement. *Lancet*. 1986;1(8476):307-310.

9. Bland JM, Altman DG. Applying the right statistics: analyses of measurement studies. *Ultrasound Obstet Gynecol*. 2003;22(1):85-93.

10. FDG-PET/CT Technical Committee. FDG-PET/CT as an Imaging Biomarker Measuring Response to Cancer Therapy, Quantitative Imaging Biomarkers Alliance (QIBA), Version 1.13, Technically Confirmed Version. QIBA, November 18, 2016. Available from: RSNA.ORG/QIBA.

11. Ferreira G, Iravani A, Hofman MS, Hicks RJ. Intra-individual comparison of (68)Ga-PSMA-11 and (18)F-DCFPyL normal-organ biodistribution [published online May 2019]. *Cancer Imaging*. 19(1):23. doi: 10.1186/s40644-019-0211-y

12. Sahakyan K, Li X, Lodge MA, et al. Semiquantitative parameters in PSMA-targeted PET imaging with [(18)F]DCFPyL: intrapatient and interpatient variability of normal organ uptake [published online May 2019]. *Mol Imaging Biol*. doi: 10.1007/s11307-019-01376-9

13. Li X, Rowe SP, Leal JP, et al. Semiquantitative parameters in PSMA-targeted PET imaging with (18)F-DCFPyL: variability in normal-organ uptake. *J Nucl Med*. 2017;58(6):942-946.

14. Sullivan DC, Obuchowski NA, Kessler LG, et al. Metrology standards for quantitative imaging biomarkers. *Radiology*. 2015;277(3):813-825.

15. Wahl RL, Jacene H, Kasamon Y, Lodge MA. From RECIST to PERCIST: evolving considerations for PET response criteria in solid tumors. *J Nucl Med*. 2009;50(Suppl 1):122S-150S.

16. Hatt M, Cheze-Le Rest C, Aboagye EO, et al. Reproducibility of 18F-FDG and 3'-deoxy-3'-18F-fluorothymidine PET tumor volume measurements. *J Nucl Med*. 2010;51(9):1368-1376.

17. Nakamoto Y, Zasadny KR, Minn H, Wahl RL. Reproducibility of common semi-quantitative parameters for evaluating lung cancer glucose metabolism with positron emission tomography using 2-deoxy-2-[18F]fluoro-D-glucose. *Mol Imaging Biol*. 2002;4(2):171-178.

18. Krak NC, Boellaard R, Hoekstra OS, Twisk JW, Hoekstra CJ, Lammertsma AA. Effects of ROI definition and reconstruction method on quantitative outcome and applicability in a response monitoring trial. *Eur J Nucl Med Mol Imaging*. 2005;32(3):294-301.

19. O JH, Lodge MA, Wahl RL. Practical PERCIST: A simplified guide to PET response criteria in solid tumors 1.0. *Radiology*. 2016;280(2):576-584.

20. Kenny LM, Contractor KB, Hinz R, et al. Reproducibility of [11C]choline-positron emission tomography and effect of trastuzumab. *Clin Cancer Res*. 2010;16(16):4236-4245.

21. Lin C, Bradshaw T, Perk T, et al. Repeatability of quantitative 18F-NaF PET: a multicenter study. *J Nucl Med*. 2016;57:1872-9.

22. Menda Y, Ponto LL, Schultz MK, et al. Repeatability of gallium-68 DOTATOC positron emission tomographic imaging in neuroendocrine tumors. *Pancreas*. 2013;42(6):937-943.

23. Kramer GM, Liu Y, de Langen AJ, et al. Repeatability of quantitative (18)F-FLT uptake measurements in solid tumors: an individual patient data multi-center meta-analysis. *Eur J Nucl Med Mol Imaging*. 2018;45(6):951-961.

24. Fendler WP, Eiber M, Beheshti M, et al. 68Ga-PSMA PET/CT: Joint EANM and SNMMI procedure guideline for prostate cancer imaging: version 1.0. *Eur J Nucl Med Mol Imaging*. 2017;44(6):1014-1024.

25. Wondergem M, van der Zant FM, Vlottes PW, Knol RJJ. Effects of Fasting on 18F-DCFPyL uptake in prostate cancer lesions and tissues with known high physiologic uptake. *J Nucl Med*. 2018;59(7):1081-1084.

26. Frings V, de Langen AJ, Smit EF, et al. Repeatability of metabolically active volume measurements with 18F-FDG and 18F-FLT PET in non-small cell lung cancer. *J Nucl Med*. 2010;51(12):1870-1877.

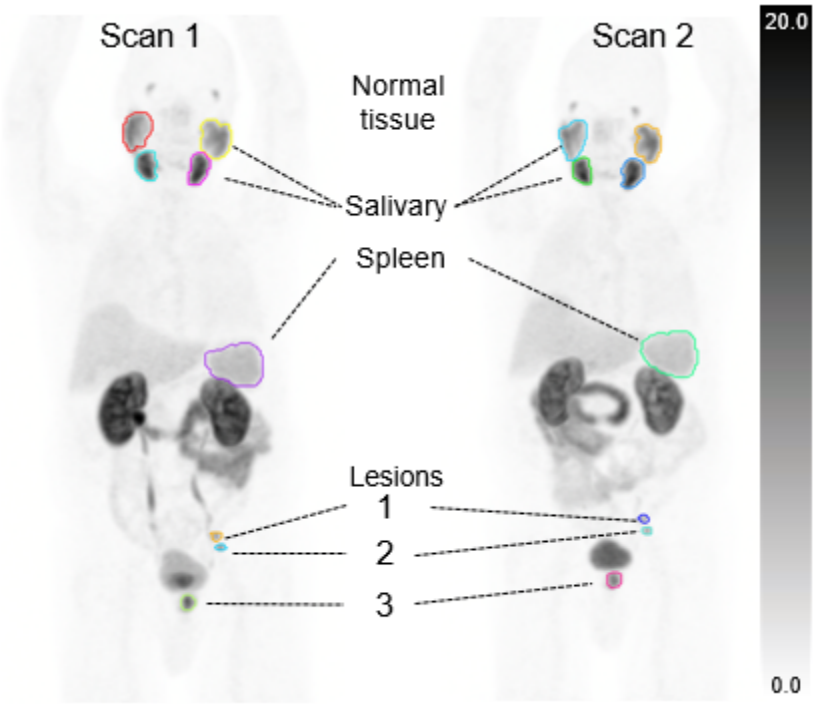

Figure 1. ^{68}Ga-PSMA-HBED-CC CC PET/CT for subject 2 for scan 1 (baseline) and scan 2 performed 2 days later showing segmentation of normal tissues (salivary glands and spleen) and sites of abnormal uptake in two left pelvic lymph nodes (1 and 2) and left prostate bed (3).

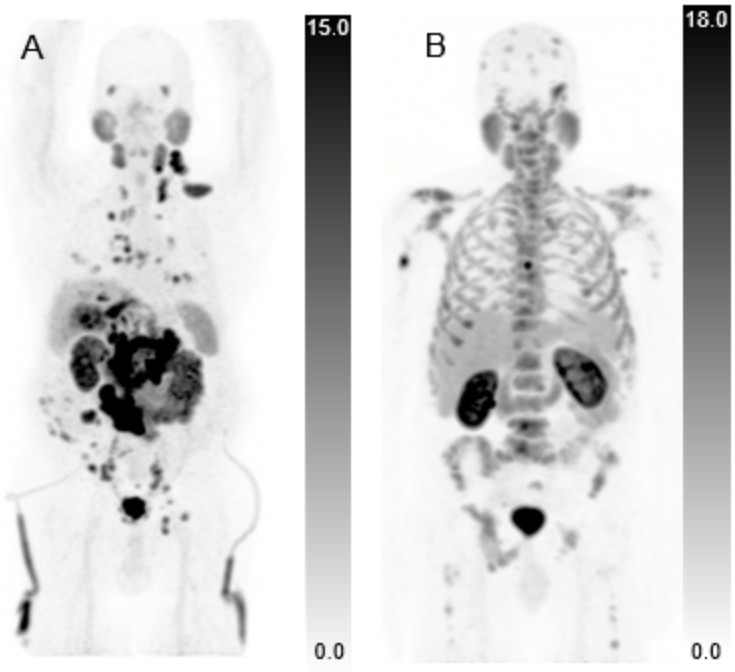

Figure 2. ^{68}Ga-PSMA-HBED-CC CC PET/CT for two subjects demonstrating different distribution of metastatic lesions. A. Predominantly soft tissue metastatic PCa is seen with visceral metastases in the lungs and liver and nodal metastases in the neck, chest, abdomen and pelvis. Percutaneous nephrostomy tubing is also visible. B. Extensive metastatic PCa is seen involving only the skeleton.

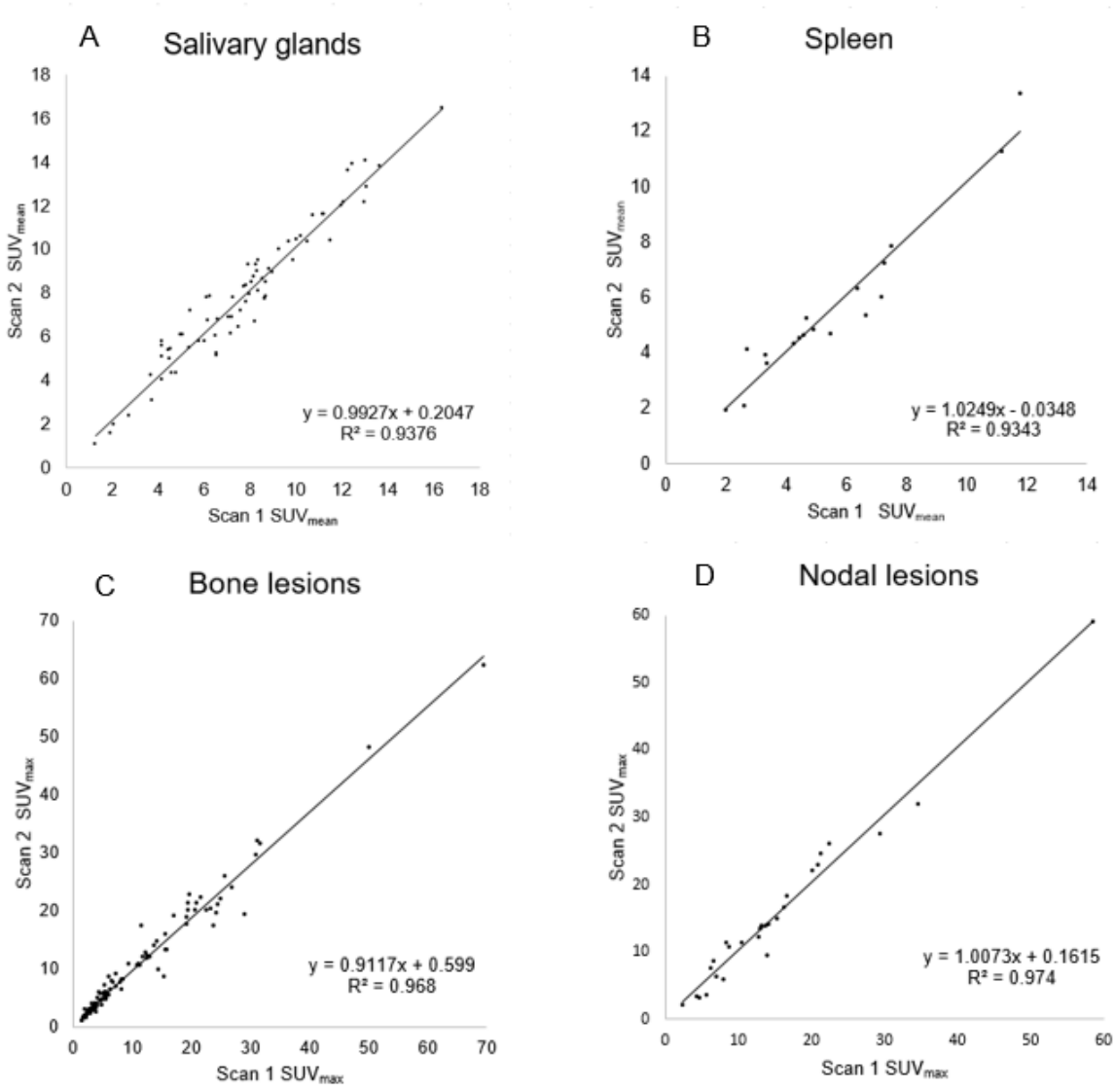

Figure 3. Correlation between test-retest measures of ^{68}Ga-PSMA-HBED-CC uptake. Plots show SUV_{mean} of normal salivary glands and spleen (A and B) and SUV_{max} for bone and nodal lesions (C and D).

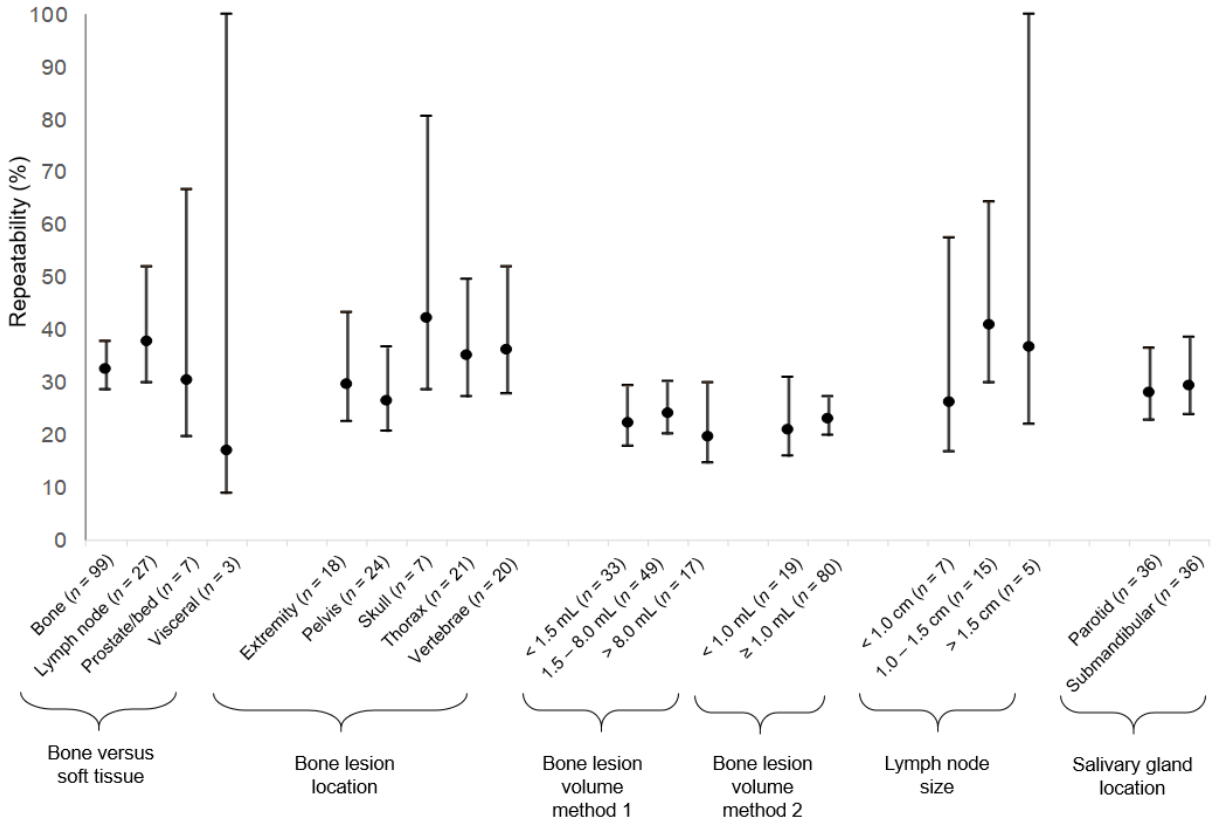

Figure 4. Comparison of SUV repeatability coefficient point estimates. The 95% confidence intervals (y-axis) show substantial overlap indicating no significant difference in repeatability for different categories of measurements (x-axis).

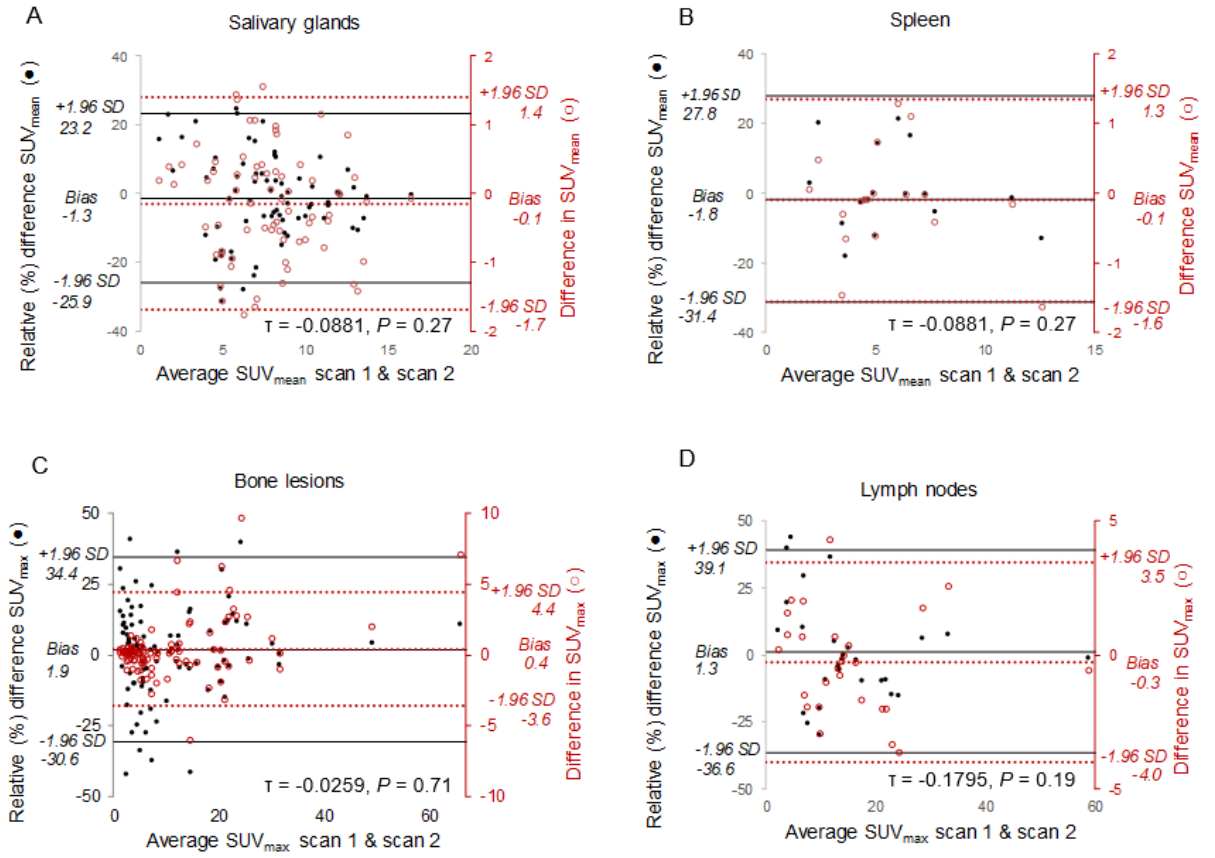

Figure 5. Bland Altman scatter plots show the difference between test-retest SUV measurements versus average lesion or organ intensity. The plots suggest no association between mean lesion or organ intensity (x-axis) and test-retest relative percentage differences (primary y-axis) based on Kendall's τ analysis. Both relative percentage difference (black ●, primary vertical axis) and absolute difference (red ○, right vertical axis) are plotted together for salivary glands (A), spleen (B), bone lesions (C), and lymph nodes (D). Horizontal lines represent upper limits of agreement (+1.96 SD), lower limits of agreement (-1.96 SD), and bias (or mean difference). Kendall's τ coefficient and p values were calculated for relative percentage difference data and are included in the field of the graphs.

(SD, standard deviation; τ, tau)

TABLE 1. Subject characteristics*

Subject	PSA within ≤ 90 days (ng/mL)	Gleason score at diagnosis	Total lesions measured	Prostate/bed	Bones	Nodes	Visceral
1	0.15	7 (4 + 5)	-	-	-	-	-
2	4.35	6 (3 + 3)	3	1	-	2	-
3	104.5	9 (4 + 5)	15	-	15	-	-
4	0.14	9 (4 + 5)	10	1	9	-	-
5	0.66	9 (5 + 4)	4	1	2	1	-
6	0.22	9 (5 + 4)	1	-	1	-	-
7	56.3	presumptive diagnosis	12	-	12	-	-
8	95.5	7 (4 + 3)	23	-	2	18	3
9	276.3	9 (4 + 5)	15	-	15	-	-
10	0.04	presumptive diagnosis	-	-	-	-	-
11	0.64	9 (4 + 5)	5	-	5	-	-
12	2.8	lymph node biopsy	12	1	8	3	-
13	40.1	10 (5 + 5)	13	1	10	2	-
14	19.7	7 (3 + 4)	2	-	2	-	-
15	2.5	bone biopsy	1	1	-	-	-
16	54.1	9 (5 + 4)	15	-	15	-	-
17	2.5	9 (5 + 4)	2	1	1	-	-
18	2.5	9 (5 + 4)	3	-	2	1	-

*PSA, prostate specific membrane antigen

TABLE 2. Repeatability data (SUV_{max})*

Organ or lesion type	wCV (%)	Symmetric RC [95% CI] (%)	Asymmetric RC	
			LRC (%)	URC (%)
Bone lesions, total (n=99)	11.7	±32.5 [28.5, 37.8]	-28.0	+38.8
Location				
Extremity (n=20)	10.7	±29.6 [22.5, 43.3]	-25.8	+34.7
Pelvic (n=25)	9.5	±26.3 [20.6, 36.6]	-23.2	+30.3
Skull (n=9)	15.2	±42.1 [28.4, 80.6]	-34.8	+53.3
Thoracic (n=23)	12.7	±35.1 [27.1, 49.7]	-29.9	+42.6
Vertebrae (n=22)	13.1	±36.2 [27.9, 51.8]	-30.7	+44.2
Lesion volume, method 1				
<1.5 mL (n=33)	8.0	±22.1 [17.8, 29.3]	-19.9	+24.8
1.5-8.0 mL (n=49)	8.7	±24.0 [20.1, 30.0]	-21.4	+27.3
>8.0 mL (n=17)	7.1	±19.6 [14.6, 29.8]	-17.8	+21.7
Lesion volume, method 2				
<1.0 mL (n=19)	7.5	±20.9 [15.8, 30.9]	-18.9	+23.3
≥1.0 mL (n=80)	8.3	±22.9 [19.9, 27.2]	-20.5	+25.9
Nodal lesions (n=27)	13.7	±37.9 [29.8, 51.9]	-31.9	+46.8
Size, long axis				
<1.0 cm (n=7)	9.4	±26.1 [16.8, 57.4]	-23.1	+30.0
1.0-1.5 cm (n=15)	14.7	±40.8 [29.8, 64.3]	-33.9	+51.3
>1.5 cm (n=5)	13.3	±36.7 [22.0, 100.0]	-31.0	+44.9
Prostate/bed (n=7)	10.9	±30.3 [19.5, 66.7]	-26.3	+35.7
Visceral lesions (n=3)	6.1	±16.9 [8.8,100.0]	-15.6	+18.5

*SUV, standardized uptake value; wCV, within-subject coefficient of variation; RC, repeatability coefficient; CI, confidence interval; LRC, lower repeatability coefficient; URC, upper repeatability coefficient

TABLE 3. Repeatability data (SUV_{mean})*

Organ or lesion type	wCV (%)	Symmetric RC [95% CI] (%)
Salivary glands, total (n=72)	8.9	±24.6 [21.1, 29.4]
Parotid glands (n = 36)	9.6	±26.5 [21.5, 34.5]
Submandibular glands (n = 36)	8.2	±22.8 [18.5, 29.8]
Spleen (n=18)	10.7	±29.6 [22.2, 44.4]
Bone lesions, total (n=99)	11.2	±30.9 [27.2, 36.0]
Location		
Extremity (n=20)	13.6	±37.8 [28.7, 55.2]
Pelvic (n=25)	9.6	±26.7 [20.8, 37.1]
Skull (n=9)	13.4	±37.0 [25.0, 70.9]
Thoracic (n=23)	11.0	±30.4 [23.5, 43.1]
Vertebrae (n=22)	9.7	±26.7 [20.7, 38.4]
Lesion volume, method 1		
<1.5 mL (n=33)	6.3	±17.4 [14.0, 23.0]
1.5-8.0 mL (n=49)	7.4	±20.5 [17.1, 25.6]
>8.0 mL (n=17)	6.2	±17.1 [12.7, 26.0]
Lesion volume, method 2		
<1.0 mL (n=19)	7.1	±19.6 [17.0, 23.2]
≥1.0 mL (n=80)	6.2	±17.1 [12.9, 25.3]
Nodal lesions (n=27)	13.2	±36.6 [28.9, 50.2]
Size, long axis		
<1.0 cm (n=7)	8.3	±23.0 [14.8, 50.7]
1.0-1.5 cm (n=15)	13.7	±37.8 [27.7, 59.7]
>1.5 cm (n=5)	17.1	±47.3 [28.4, 100.0]
Prostate/bed (n=7)	8.3	±22.9 [14.8, 50.4]
Visceral lesions (n=3)	2.7	±7.6 [4.0, 47.8]

*SUV, standardized uptake value; wCV, within-subject coefficient of variation; RC, repeatability coefficient; CI, confidence interval; LRC, lower repeatability coefficient; URC, upper repeatability coefficient

Supplemental Table 1. Treatment regimen at the time of scan 1 and scan 2*

Subject	Systemic therapy
1	Anti-androgen (bicalutamide), GnRH analog (leuprolide), denosumab
2	Anti-androgen (bicalutamide), GnRH analog (triptorelin)
3	Anti-androgen (enzalutamide), GnRH analog (leuprolide)
4	Docetaxeol, GnRH analog (leuprolide), denosumab
5	GnRH analog (triptorelin), zolendronate
6	GnRH analog (triptorelin), denosumab
7	Anti-androgen (enzalutamide), GnRH analog (triptorelin), zolendronate
8	GnRH analog (triptorelin), denosumab
9	Anti-androgen (enzalutamide), GnRH analog (leuprolide), denosumab
10	GnRH analog (leuprolide), denosumab
11	GnRH analog (leuprolide),
12	GnRH analog (leuprolide), denosumab
13	Anti-androgen (enzalutamide), GnRH analog (leuprolide), denosumab
14	(bilateral orchiectomy)

15	Abiraterone, GnRH analog (leuprolide)
16	Anti-androgen (enzalutamide), GnRH analog (leuprolide), denosumab
17	GnRH analog (leuprolide)
18	GnRH analog (leuprolide)

*GnRH, gonadotropin-releasing hormone

SUPPLEMENTAL TABLE 2. Repeatability between scanner type for SUV_{max}*†

Organ or lesion	Siemens mCT (n = 11 subjects)		Siemens Biograph Truepoint (n = 7 subjects)		
	SUV_{max}		SUV_{max}		
	n	wCV (%)	n	wCV (%)	*P*
Parotid glands	22	9.7	14	9.3	0.64
Submandibular glands	22	10.7	14	9.3	0.55
Spleen	11	10.9	7	7.1	0.52
Bone lesions, total	51	11.4	48	12.1	0.28
Location					
Extremity	12	11.0	8	8.9	0.73
Pelvic	12	6.6	13	11.2	0.06
Skull	6	11.2	3	16.2	0.60
Thoracic	11	12.0	12	12.9	0.47
Vertebrae	10	14.3	12	10.3	0.66
Nodal lesions	21	10.9	6	9.3	0.85
Prostate/bed	4	12.0	3	5.6	0.21

*SUV, standardized uptake value; wCV, within-subject coefficient of variation

†Visceral lesions were excluded from analysis due to their small number and only being present in the cohort imaged on the mCT.

SUPPLEMENTAL TABLE 3. Repeatability between scanner type for SUV_{mean}*†

Organ or lesion	Siemens mCT (n = 11 subjects)		Siemens Biograph Truepoint (n = 7 subjects)		
	SUV_{mean}		SUV_{mean}		
	n	wCV (%)	n	wCV (%)	*P*
Parotid glands	22	9.4	14	9.3	0.97
Submandibular glands	22	8.0	14	10.1	0.31
Spleen	11	12.1	7	6.1	0.35
Bone lesions, total	51	10.6	48	10.4	0.28
Location					
Extremity	12	15.4	8	10.7	0.36
Pelvic	12	9.9	13	10.1	0.59
Skull	6	8.3	3	13.4	0.51
Thoracic	11	6.4	12	8.5	0.29
Vertebrae	10	9.5	12	9.0	0.86
Nodal lesions	21	11.4	6	9.7	0.95
Prostate/bed	4	4.8	3	9.2	0.11

*SUV, standardized uptake value; wCV, within-subject coefficient of variation

†Visceral lesions were excluded from analysis due to their small number and only being present in the cohort imaged on the mCT